ISSN 0003-6838, Applied Biochemistry and Microbiology, 2019, Vol. 55, No. 5, pp. 489–494. © Pleiades Publishing, Inc., 2019.

Increased Productivity and Antifreeze Activity of Ice-binding Protein from *Flavobacterium frigoris* PS1 Produced using *Escherichia coli* as Bioreactor

E. J. Kim[a, b], J. E. Kim[a, c], J. S. Hwang[b, d], I.-C. Kim[a], S. G. Lee[b, d], S. Kim[a], J. H. Lee[b, d], and S. J. Han[a, b, *]

[a] *Division of Polar Life Sciences, Korea Polar Research Institute, KIOST, Incheon, 21990 South Korea*
[b] *Department of Polar Sciences, University of Science and Technology, Incheon, 21990 South Korea*
[c] *Department of Pharmacy, Graduate School, Sungkyunkwan University, Suwon, 16419 South Korea*
[d] *Unit of Polar Genomics, Korea, Polar Research Institute, Incheon, 21990 South Korea*
**e-mail: hansj@kopri.re.kr*

Received November 12, 2018; revised March 3, 2019; accepted April 22, 2019

Abstract—Ice-binding proteins (IBPs) inhibit the growth and recrystallization of intracellular ice, enabling polar organisms to survive at subzero temperatures. IBPs are promising materials in biomedical applications such as cryopreservation and the hypothermic storage of cells, tissues, and organs. In this study, recombinant IBP from the antarctic bacterium *Flavobacterium frigoris* PS1 (FfIBP) was produced by *Escherichia coli* used as bioreactor, to examine the feasibility of scale-up. Oxygen transfer was the most important factor influencing cell growth and FfIBP production during pilot-scale fermentation. The final yield of recombinant FfIBP produced by *E. coli* harboring the pET28a-FfIBP vector system was 1.6 g/L, 3.8-fold higher than that from the previously published report using pCold I-FfIBP vector system, and its thermal hysteresis activity was 2.5°C at 9.7 μM. This study demonstrates the successful pilot-scale production of FfIBP.

Keywords: Antarctica, ice-binding protein, *Flavobacterium frigoris*, pilot-scale fermentation, thermal hysteresis
DOI: 10.1134/S0003683819050077

Although the Arctic and the Antarctic are the coldest, windiest, and driest regions on Earth, they are the habitats of a variety of microorganisms. Psychrophiles and psychrotrophs are cold-tolerant organisms that can grow at low temperatures. They produce active biochemical substances and increase the polyunsaturated fatty acid content to improve membrane fluidity at low temperatures [1]. The sea and freshwater organisms inhabiting the Antarctic and Arctic are consistently exposed to low temperatures (sea water; −1.9–2.0°C, fresh water; 0–5°C) [2]. Ice binding proteins (IBPs) have been found in various psychrophilic and psychrotrophic organisms living at subzero temperatures, such as bacteria [1, 2], fungi [3–5], diatoms [6], plants [7–9], insects [10, 11], and fish [12]. IBPs, also called antifreeze proteins (AFPs), play key roles in inhibiting ice crystal growth and its recrystallization by adsorbing on the ice surface [8, 13]. They prevent cell injury and death due to intracellular ice formation and frozen cell membranes. Many antifreeze materials exist besides IBPs, such as ethylene glycol [14], dimethyl sulfoxide (DMSO) [15], poly(vinyl alcohol) [16], metallohelices [17], and polysaccharides [18]. Ethylene glycol can be used to cryopreserve biological tissues and organs [14], and DMSO is used in biology to decrease ice formation. However, ethylene glycol is toxic when decomposed in the body [19], and DMSO induces cell lysis and apoptosis by increasing intracellular calcium levels [20]; the others mentioned do not yet have practical uses. Unlike these chemicals, IBPs obtained from natural organisms have low or no toxicity, and have been applied in biomedical research and other applications, such as tissues and organ cryopreservation, food preservation, and skin protection [21]. However, extracting IBPs directly from organisms has quantitative limitations and is cost-inefficient. Industrial application will require the heterologous expression of IBPs using large-scale bioreactors.

Our research team has previously investigated the properties of several IBPs from antarctic and arctic organisms, including *Leucosporidium* IBP (LeIBP, recently reclassified genus as *Glaciozyma* sp. AY30), FfIBP, and Type-III AFP [5, 22–25]. FfIBP was isolated from the bacterium *Flavobacterium frigoris* PS1, which inhabits antarctic marine ice. It has a higher thermal hysteresis (TH) activity than LeIBP, and has been produced in *Escherichia coli* using a cold shock induction system with the pCold I vector. Production of FfIBP using the pCold I vector system was advantageous in terms of protein stability, but it had the disadvantage of a long incubation time (over 50 h to reach a cell concentration of 6.3 g/L and protein production

of 0.42 g/L) [26]. The pCold I vector system increased target protein expression at lower temperatures, but *E. coli* had a lower cell growth rate at 15°C than at 37°C [27]. In this study, to increase the productivity of FfIBP, the expression gene was inserted into the pET28a vector and *E. coli* expressing recombinant FfIBP was cultured in modified R medium at 37°C. Using 7 L fermenter, we compared FfIBP production at various IPTG concentrations. Then, pilot-scale fermentations were performed in 30 L fermenter, and FfIBP production and antifreeze activity were evaluated.

MATERIALS AND METHODS

Strains and plasmids. For recombinant *E. coli* expression, the gene encoding FfIBP (amino acids 29–276) was obtained from *F. frigoris* PS1, isolated from antarctic sea ice [28], and amplified by PCR using the forward primer (5'-CGATAACATATGTCTCTATCAGTTGCAAAT-3') and the reverse primer (5'-CGATAACTCGAGTCATTGTGGTATGGTAACGGT-3'). Amplified fragments were digested with NdeI and XhoI, and cloned into the pET28a vector (Invitrogen, USA). The constructed plasmid was transformed into *E. coli* strain BL21 (DE3) (Promega, USA) for expression.

Media and culture conditions. A seed culture was prepared in Luria-Bertani (LB) medium (g/L): tryptone – 10.0; yeast extract – 5.0 and NaCl – 10.0 at 37°C. Cultivation in the 7 L fermenter was performed with 4 L of modified R medium(g/L): $(NH_4)_2HPO_4$ – 4.0; KH_2PO_4 – 13.5; citric acid – 1.7; bacto- tryptone – 10.0; yeast extract – 20.0; lactose – 20.0; glycerol – 50.0; $MgSO_4 \cdot 7H_2O$ – 1.2 supplemented with trace metal elements, 5.0 mL/L and adjusted to pH 7.0 before sterilization. Trace metal elements consisted of 10.0 g $FeSO_4 \cdot 7H_2O$, 2.0 g $CaCl_2 \cdot 2H_2O$, 2.25 g $ZnSO_4 \cdot 7H_2O$, 0.5 g $MnSO_4 \cdot 4–5H_2O$, 1.0 g $CuSO_4 \cdot 5H_2O$, 0.1 g $(NH_4)_6Mo_7O_{24} \cdot 7H_2O$, 0.23 g $Na_2B_4O_7 \cdot 10H_2O$ dissolved in 1 L distilled water with 5.0 mL of 35% HCl. The seven L fermenter (Kobiotech, Korea) was used to compare protein production induced by different IPTG (Elpis Biotech, Korea) concentrations. During incubation, air was added at 5 L/min. When the OD_{600} was 8 ± 1, equivalent to 2.5 g DCW/L, 0.1 mM, 0.5 mM, or 1.0 mM IPTG was added to induce protein expression. For pilot-scale cultivation, 20 L of modified R medium was used in 30 L fermenter (Biotron, Korea) and 2 L of LB medium was used for the seed culture. The dissolved oxygen level of the 20 L culture was maintained by adjusting the air/pure oxygen supply to ~25 L/min. The agitation speed varied between 100–500 rpm.

Analytical methods. To determine the growth of *E. coli*, samples were removed periodically, and the OD_{600} and DCW were measured. The OD_{600} was measured with a UV/VIS spectrophotometer (Ultrospec 3300 pro, Amersham Biosciences, USA). The DCW was determined by centrifuging 1 mL of culture broth at 16000 × *g* for 2 min, washing twice with distilled water, drying at 60°C for 120 h, and measuring the weight. OD_{600} and DCW values were determined in triplicate, and the ratio of DCW to OD_{600} was 0.31.

To confirm protein expression, 1 mL of each periodically collected sample was adjusted to an OD_{600} of 1, and centrifuged to remove the medium and obtain cell pellets. The cells were suspended in 50 μL of lysis buffer (50 mM NaH_2PO_4, 300 mM NaCl, and 5 mM imidazole, pH 7.9) and 15 μL was used for analysis. Samples were boiled for 5 min and analyzed by SDS-PAGE using 12% polyacrylamide gels. The gels were stained with Coomassie brilliant blue R-250 (Bio-Rad, USA). The FfIBP concentration was calculated by comparing the band density with a 1 g/L BSA as a standard, using ImageJ version 1.51K (National Institutes of Health, USA).

FfIBP purification. FfIBP was purified from 20 L culture after a 24-h induction period. The sample was centrifuged at 3000 *g* for 10 min at 4°C. The supernatant was removed and the pellet was collected for protein purification. The bacterial pellet, containing overexpressed His-tagged FfIBP, was lyzed in lysis buffer with sonication (pulse 35%, pulse on/off 1/5 s) at 4°C. The lysate was clarified by centrifugation (11000 *g* for 20 min at 4°C), loaded onto a Ni-NTA resin (Elpis Biotech, Korea) column pre-equilibrated with binding buffer (20 mM Tris-HCl, 0.5 M NaCl, and 5 mM imidazole, pH 7.9) and washed with 10-bed volumes of wash buffer (20 mM Tris-HCl, 0.5 mM NaCl, and 60 mM imidazole, pH 7.9). The bound FfIBP was eluted with elution buffer (10 mM Tris-HCl, 0.25 M NaCl, and 0.5 M imidazole, pH 7.9). To obtain highly purified proteins, fractions were collected from the column, and among them, the one with highest purity was selected. The final eluate of the selected fraction was dialyzed against 50 mM Tris-HCl (pH 8.0) containing 150 mM NaCl and concentrated using a 10-kDa centrifugal filter (Amicon Ultra Centrifugal filter, Millipore, USA). The concentration of purified protein was determined using the Bradford method for protein quantitation (Bradford reagent, Sigma-Aldrich, USA) [29].

Determination of TH activity. The TH activity of FfIBP was measured using a nanoliter osmometer (Otago Osmometers, New Zealand). The purified FfIBP concentration was adjusted to 0.60, 1.21, 2.43, 4.87, and 9.70 μM, and TH activity was measured in triplicate. Ice crystal morphology was captured with a digital camera (Canon, Japan) connected to an optical microscope (BX53, Olympus, Japan).

Ice Recrystallization inhibition assay. Recrystallization inhibition (RI) analysis was performed as previously described [24]. Purified FfIBP samples were mixed with 60% sucrose solution in a 1 : 1-ratio, and 3.8 μL of the mixed sample solution was added between two glass cover slips (16 mm diameter). The overlapped round glasses were pre-chilled on the sur-

(a)

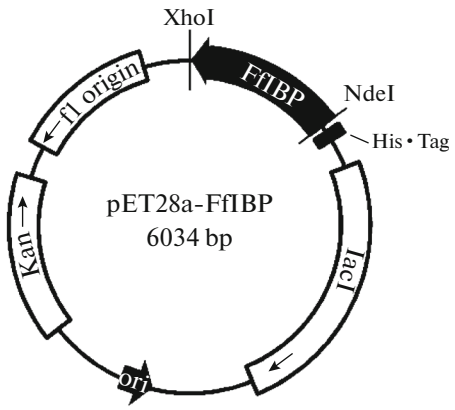

(b)

SLSVANSTYETTALNSQKSSTDQPNSGSKSGQTLDLVNLGVAANFAILSKTGITD
VYKSAITGDVGASPITGAAILLKCDEVTGTIFSVDAAGPACKITDASRLTTAVGDM
QIAYDNAAGRLNPDFLNLGAGTIGGKTLTPGLYKWTSTLNIPTDITISGSSTDVWI
FQVAGNLNMSSAVRITLAGGAQAKNIFWQTAGAVTLGSTSHFEGNILSQTGIN
MKTAASINGRMMAQTAVTLQMNTVTIPQ

Fig. 1. Plasmid map of the pET28a-FfIBP expression construct (a). Amino acid sequence of FfIBP from *F. frigoris* PS1 (b).

face at 4°C. After 1 min, the sample was cooled to −70°C at a rate of 60°C/min on a circulating cooling stage (THMS600 stage, Linkam Scientific Instruments, England) and then incubated for 60 min at −6°C. Ice recrystallization in cover glasses was analyzed by using a microscope (Olympus BX51), and images were recorded using a DP71 CCD camera (Olympus, Japan) every 10 min.

RESULTS AND DISCUSSION

Construction of FfIBP-expression vector. The *IBP* gene from *F. frigoris* PS1, which was isolated from antarctic sea ice and sequenced [28], was cloned into an *E. coli* expression vector, the recombinant protein was overexpressed in *E. coli* and purified using single-step metal-chelate chromatography. For IBP production, the FfIBP cDNA (residues 29–276; the first 28 residues, which predicted a signal-peptide sequence, were removed) was subcloned into the pET28a vector (5.369 bp), which contained a kanamycin-resistance gene for selection (Fig. 1a). The molecular weight of the expressed FfIBP was approximately 25.7 kDa (Fig. 1b).

FfIBP expression after induction with varying IPTG concentrations. FfIBP was produced in *E. coli* in 7 L jar fermenter containing 4 L medium. To investigate the effects of IPTG concentration on the FfIBP yield, 0.1, 0.5, and 1.0 mM IPTG was added to the cultures. The *E. coli* cell growth (determined as the g dry cell weight (DCW)/L) and yield of recombinant FfIBP were monitored. After 13 h induction with 0.1, 0.5, and 1.0 mM IPTG, the cell concentrations reached 15.9, 14.9, and 12.9 g/L, respectively (Fig. 2a), showing an inverse trend. According to Kim et al. [21], LeIBP productivity in *E. coli* supplemented with 0.1 mM IPTG was higher than that with 1 mM IPTG in a 7-L fermenter. In 2002, Malakar and Venkatesh [30] reported that high IPTG concentrations inhibited cell growth. However, in this study, 19.5 h after induction, all experimental groups reached cell concentrations of ~17.6 g/L, with no significant differences between different IPTG concentrations (Fig. 2a). Twenty four h induction in the presence of 0.1, 0.5, and 1.0 mM IPTG resulted in 1.6, 1.6, and 1.5 g/L FfIBP yield, respectively (Fig. 2b). These results indicate that reducing the IPTG concentration to 0.1 mM did not significantly decrease FfIBP production. Since lower IPTG concentrations decrease production cost [30], we used this concentration in the pilot-scale production of FfIBP.

Production of FfIBP in 30 L fermenter. The cell concentration reached 18 g DCW/L (24 h after induction) in 4 L laboratory scale fermentation in 7 L fermenter with only air supplied. Oxygen limitation was observed when the culture volume 5-fold increased from 4 to 20 L, and pure oxygen was required to grow cells to 14.2 g DCW/L (21 h after induction) in a pilot 20 L culture in 30 L fermenter (Fig. 3a). Oxygen supply is a known key factor limiting growth during the production of recombinant protein in *E. coli* [31]. The FfIBP band was observed at approximately 24 kDa by

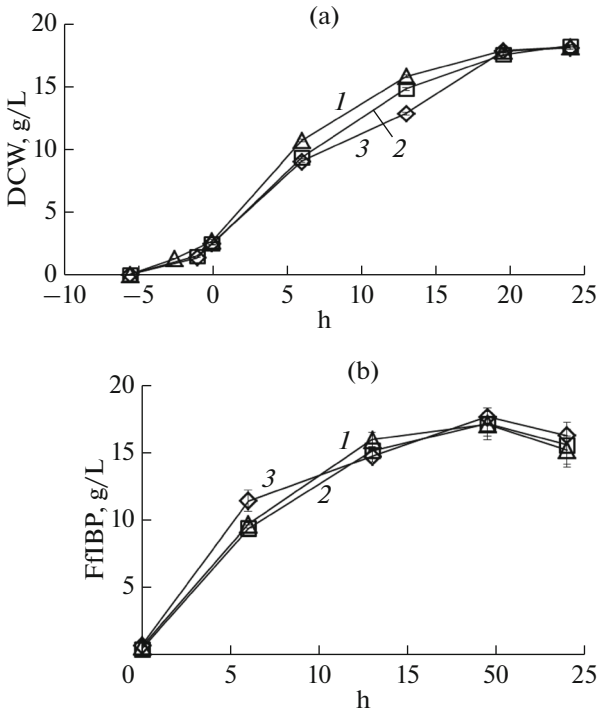

Fig. 2. FfIBP expression induced in the presence of various IPTG concentrations (*1*—0.1, *2*—0.5, and *3*—1.0 mM) in 7 L fermenter. (a)—DCW dependence on time after IPTG induction. (b)—FfIBP production calculated by comparing the band density with that for BSA standard and depending on time after IPTG induction.

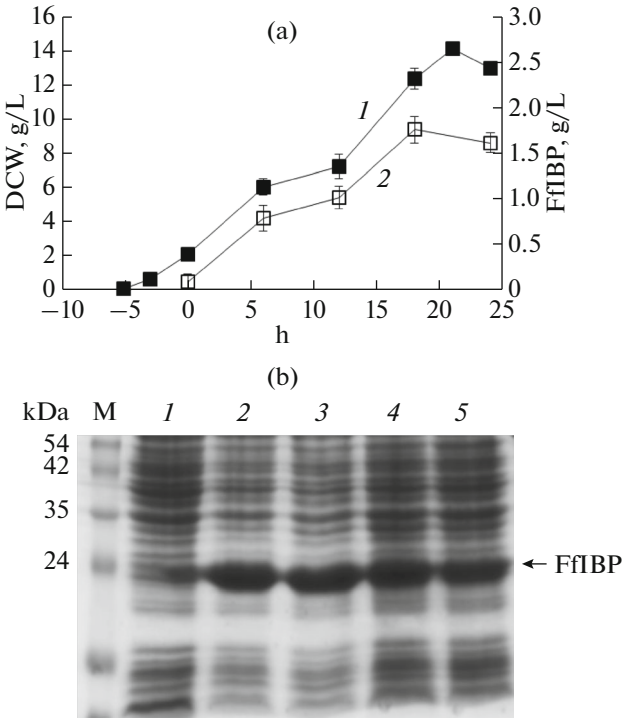

Fig. 3. DCW (*1*) and FfIBP concentration (*2*) depending on time after IPTG induction in 30 L scale fermenter (a). (FfIBP was produced in *E. coli* at 37°C after 24 h induction with 0.1 mM IPTG). Visualization of FfIBP expression by SDS-PAGE (b). Lane M: protein markers; lanes *1*–*5*: after 0, 6, 12, 18, and 24 h induction, respectively.

SDS-PAGE after 6 h induction (Fig. 3b). Individual band intensities were quantified, and the calculated FfIBP yield was the highest (1.8 g/L) after 18 h induction, and 1.6 g/L after 24 h induction, whereas the FfIBP yield produced by *E. coli* with the pCold I vector system in 20 L culture was 0.42 g/L [26]. We therefore obtained more than 3.8-fold increase of the FfIBP level by changing the expression vector system from pCold I to pET28a. In addition, the incubation time was shortened to 24 h. In comparison with yield of the recombinant FfIBP produced in *P. pastoris*, which yielded 75 mg/L in 4 L culture [25], the production level increased 21-fold in this study by changing the expression host (Table 1). In this study, the yield of FfIBP produced in 30 L fermenter using *E. coli* was 1.6 g/L, similar to that produced in a 7 L fermenter. These results indicate successful scale-up from 4 to 20 L.

FfIBP purification and TH activity assay. Purified and concentrated FfIBP was quantified by the Bradford method, and its concentration was observed to be 9.7 μM (250 μg/mL). The purified FfIBP was serially diluted and visualized by SDS-PAGE (Fig. 4a). We examined the effect of the purified FfIBP on the temperature gap between the melting and freezing points using a nanoliter osmometer. The TH activity of 9.7 μM FfIBP was 2.5°C, identical to that of FfIBP

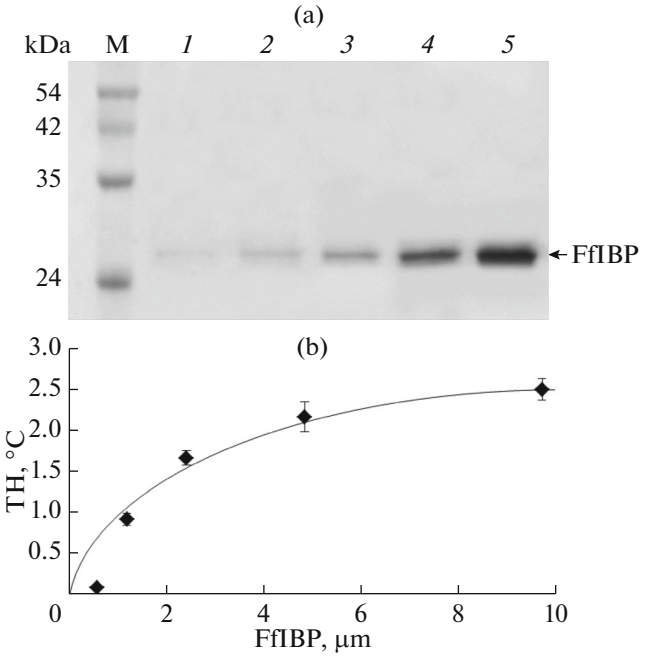

Fig. 4. Visualization of FfIBP produced in 30 L jar fermenter using SDS-PAGE (a). (FfIBP was purified after 24 h induction). Lane M: protein markers; lanes *1*–*5*: 0.6, 1.21, 2.43, 4.85, and 9.70 μM of FfIBP, respectively. Thermal hysteresis activity of 0.6, 1.21, 2.43, 4.85, and 9.70 μM FfIBP (b).

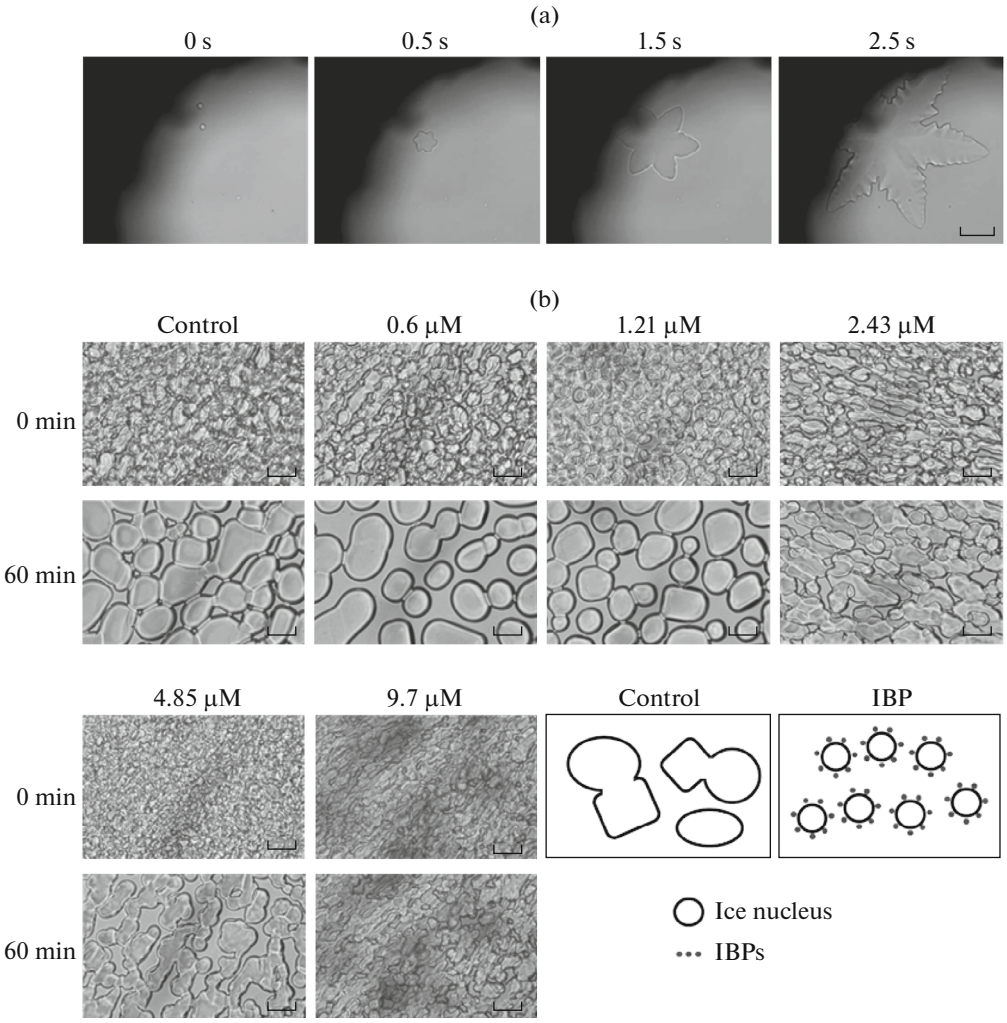

Fig. 5. Ice crystal morphology and ice RI assay. Ice crystal growth in solution containing FfIBP (2.43 μM) at the freezing point (a). Scale bar, 100 μm. Inhibition of ice recrystallization by FfIBP (b). The control (BSA protein, 30 μM) was used for RI assay. RI activity is shown in the photographs at 5 different concentrations of FfIBP. Scale bar, 20 μm.

expressed in *E. coli* with the pCold I vector system in a previous study (Fig. 4b) [24].

Ice crystal morphology and ice recrystallization inhibition assay. Ice crystals forming in the presence of FfIBP had a hexagonal shape, and the crystal burst was along the a-axis plane (Fig. 5a) [24]. The crystal type induced by FfIBP was similar to those that grow along the a-axis in AFP1 from the yeast *Glaciozyma antarctica* PI12 and ChloroIBP from the microalga *Chloromonas* sp., while LeIBP, type I, II, and

Table 1. Comparison of recombinant FfIBP produced in different bioreactors

Expression host [vector]	Production conditions*	Protein yield, g/L	TH, °C [concentration]	Reference
E. coli [pCold I]	20 L, modified R medium, 0.5 mM IPTG, 15°C	0.42 (band density)	1.53 [10 μM]	[26]
P. pastoris [pPICZαA]	4 L, fermentation basal medium, methanol, 30°C	0.075 (Bradford assay)	2.6 [110 μM]	[25]
E. coli [pET28a]	20 L, modified R medium, 0.1 mM IPTG, 37°C	1.6 (band density)	2.5 [9.7 μM]	This study
E. coli [pET28a]	4 L, modified R medium, 0.1 mM IPTG, 37°C	1.5 (band density)	NS**	This study

* Culture volume, culture medium, induction method, and temperature.
** NS, not specified.

III AFPs build the ice crystals that grow along the c-axis [23, 32, 33]. The recrystallization inhibition (RI) activity of FfIBP was measured and formation and fusion of ice nuclei are shown in Fig. 5b. FfIBP inhibited the recrystallization of ice at −6°C for 60 min in contrast with the control (BSA). RI activity assays were conducted with 5 different concentrations of FfIBP. At a concentration FfIBP of 2.43 μM or more, the size of ice crystals maintained small even after 1 h of freezing, indicating that RI activity was expectedly present (Fig. 5b).

Because IBPs can reduce or suppress the physical damage to living cells and tissues induced by ice crystals at subzero temperatures, these proteins are promising tools in biomedical applications. In this study, FfIBP, an IBP derived from antarctic *F. frigoris* PS1, was produced in 7 and 30 L scale fermenters using *E. coli* as bioreactor. There were no significant differences in protein productivity after 0.1, 0.5, and 1.0 mM IPTG inductions. Twenty L pilot scale fermentation performed with modified R medium, 0.1 mM IPTG and oxygen supply (~25 L/min) for 24 h resulted in 1.6 g/L FfIBP production with a TH activity of 2.5°C at 9.7 μM. These results can be applied to the large-scale production and biotechnological application of recombinant IBPs.

ACKNOWLEDGMENTS

We thank Prof. E.S. Jin (Hanyang University) for her generous support and use of facilities, and Mr. M.J. Kim (Hanyang University) for his technical assistance in the use of the osmometer. This research was supported by research projects (PE18180 and PE18210) from the Korea Polar Research Institute, Incheon, Korea.

COMPLIANCE WITH ETHICAL STANDARDS

The authors declare that they have no conflict of interest. This article does not contain any studies involving animals or human participants performed by any of the authors.

REFERENCES

1. Gilbert, J.A., Hill, P.J., Dodd, C.E., and Laybourn-Parry, J., *Microbiology*, 2004, vol. 150, no. 1, pp. 171–180.
2. Kawahara, H., Iwanaka, Y., Higa, S., Muryoi, N., Sato, M., Honda, M., et al., *Cryo Lett.*, 2007, vol. 28, no. 1, pp. 39–49.
3. Hoshino, T., Kiriaki, M., Ohgiya, S., Fujiwara, M., Kondo, H., Nishimiya, Y., et al., *Can. J. Bot.*, 2003, vol. 81, no. 12, pp. 1175–1181.
4. Kondo, H., Hanada, Y., Sugimoto, H., Hoshino, T., Garnham, C.P., Davies, P.L., and Tsuda, S., *Proc. Natl. Acad. Sci. U. S. A.*, 2012, vol. 109, no. 24, pp. 9360–9365.
5. *Cold–Adapted Yeasts. Biodiversity, Adaptation Strategies and Biotechnological Significance,* Buzzini, P. and Rosa Margesin, R., Eds., Heidelberg, Germany: Springer–Verlag, 2014.
6. Janech, M.G., Krell, A., Mock, T., Kang, J.S., and Raymond, J.A., *J. Phycol.*, 2006, vol. 42, no. 2, pp. 410–416.
7. Smallwood, M., Worrall, D., Byass, L., Elias, L., Ashford, D., Doucet, C.J., et al., *Biochem. J.*, 1999, vol. 340, no. 2, pp. 385–391.
8. Griffith, M. and Yaish, M.W.F., *Trends Plant Sci.*, 2004, vol. 9, no. 8, pp. 399–405.
9. Middleton, A.J., Brown, A.M., Davies, P.L., and Walker, V.K., *FEBS Lett.*, 2009, vol. 583, no. 4, pp. 815–819.
10. Duman, J.G., Bennett, V., Sformo, T., Hochstrasser, R., and Barnes, B.M., *J. Insect Physiol.*, 2004, vol. 50, no. 4, pp. 259–266.
11. Hakim, A., Nguyen, J.B., Basu, K., Zhu, D.F., Thakral, D., Davies, P.L., et al., *J. Biol. Chem.*, 2013, vol. 288, no. 17, pp. 12295–12304.
12. DeVries, A.L., Komatsu, S.K., and Feeney, R.E., *J. Biol. Chem.*, 1970, vol. 245, no. 11, pp. 2901–2908.
13. Chao, H.M., Davies, P.L., and Carpenter, J.F., *J. Exp. Biol.*, 1996, vol. 199, no. 9, pp. 2071–2076.
14. Chi, H.J., Koo, J.J., Kim, M.Y., Joo, J.Y., Chang, S.S., and Chung, K.S., *Hum. Reprod.*, 2002, vol. 17, no. 8, pp. 2146–2151.
15. Akkok, C.A., Liseth, K., Hervig, T., Ryningen, A., Bruserud, O., and Ersvaer, E., *Cytotherapy*, 2009, vol. 11, no. 6, pp. 749–760.
16. Burkey, A.A., Riley, C.L., Wang, L.K., Hatridge, T.A., and Lynd, N.A., *Biomacromolecules*, 2018, vol. 19, no. 1, pp. 248–255.
17. Mitchell, D.E., Clarkson, G., Fox, D.J., Vipond, R.A., Scott, P., and Gibson, M.I., *J. Am. Chem. Soc.*, 2017, vol. 139, no. 29, pp. 9835–9838.
18. Dreischmeier, K., Budke, C., Wiehemeier, L., Kottke, T., and Koop, T., *Sci. Rep.*, 2017, vol. 7, p. 41890.
19. Moore, M.M., Kanekar, S.G., and Dhamija, R., *Radiol. Case Rep.*, 2008, vol. 3, no. 1, pp. 122.
20. Best, B.P., *Rejuv. Res.*, 2015, vol. 18, no. 5, pp. 422–436.
21. Kim, E.J., Lee, J.H., Lee, S.G., and Han, S.J., *KSBB J.*, 2017, vol. 32, no. 4, pp. 300–305.
22. Lee, J.H., Park, A.K., Do, H., Park, K.S., Moh, S.H., Chi, Y.M., et al., *J. Biol. Chem.*, 2012, vol. 287, no. 14, pp. 11460–11468.
23. Lee, J.H., Lee, S.G., Do, H., Park, J.C., Kim, E., Choe, Y.H., et al., *Appl. Microbiol. Biot.*, 2013, vol. 97, no. 8, pp. 3383–3393.
24. Do, H., Kim, S.J., Kim, H.J., and Lee, J.H., *Acta Crystallogr. D*, 2014, vol. 70, no. 4, pp. 1061–1073.
25. Kim, E.J., Lee, J.H., Lee, S.G., and Han, S.J., *Prep. Biochem. Biotech.*, 2017, vol. 47, no. 3, pp. 299–304.
26. Kim, E.J., Lee, J.H., Lee, S.G., and Han, S.J., *KSBB J.*, 2015, vol. 30, no. 6, pp. 345–349.
27. Farewell, A., and Neidhardt, F.C., *J. Bacteriol.*, 1998, vol. 180, no. 17, pp. 4704–4710.
28. Raymond, J.A. and Kim, H.J., *Plos One*, 2012, vol. 7, no. 5. e35968.
29. Bradford, M.M., *Anal. Biochem.*, 1976, vol. 72, no. 1–2, pp. 248–254.
30. Malakar, P. and Venkatesh, K.V., *Appl. Microbiol. Biot.*, 2012, vol. 93, no. 6, pp. 2543–2549.
31. Junker, B.H., *J. Biosci. Bioeng.*, 2004, vol. 97, no. 6, pp. 347–364.
32. Doxey, A.C., Yaish, M.W., Griffith, M., and McConkey, B.J., *Nat. Biotechnol.*, 2006, vol. 24, no. 7, pp. 852–855.
33. Bar-Dolev, M., Celik, Y., Wettlaufer, J.S., Davies, P.L., and Braslavsky, I., *J. R. Soc. Interface*, 2012, vol. 9, no. 77, pp. 3249–3259.